Journal of
Materials Chemistry A

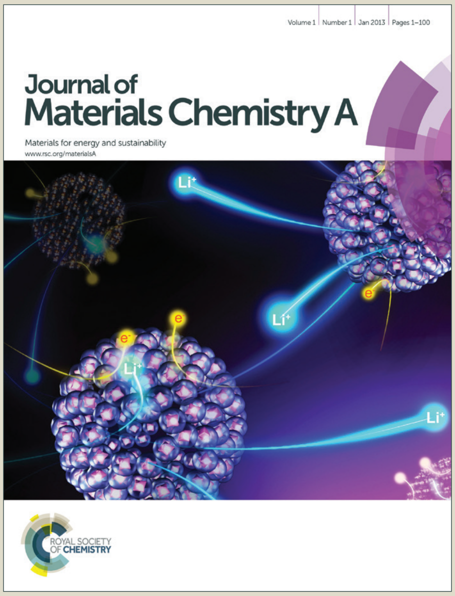

ROYAL SOCIETY
OF CHEMISTRY

www.rsc.org/materialsA

Journal Name

Journal of Materials Chemistry A

Dynamic Article Links ►

Cite this: DOI: 10.1039/c0xx00000x

www.rsc.org/xxxxxx

Paper

Inkjet printing for direct micropatterning of superhydrophobic surface: toward biomimetic fog harvesting surfaces

Lianbin Zhang,[a] Jinbo Wu,[a] Mohamed Nejib Hedhili,[b] Xiulin Yang[a] and Peng Wang*[a]

Received (in XXX, XXX) Xth XXXXXXXXX 20XX, Accepted Xth XXXXXXXXX 20XX

DOI: 10.1039/b000000x

Motivated by the efficient fog harvesting behavior of the *Stenocara* beetles in Namib Desert, the preparation of biomimetic superhydrophobic surface with hydrophilic micro-sized patterns is highly desired, but direct and facile method (i.e., one-step and thus mask-free) of producing such is still nonexistent up to this point. Herein, we report a bio-inspired method for direct preparation of stable superhydrophilic micropatterns onto superhydrophobic surface based on a facile inkjet printing technology. By directly inkjet printing a mussel-inspired ink of dopamine solution with delicately optimized solution composition, stable Wenzel's microdroplets of dopamine solution with well-defined micropatterns are obtained onto the superhydrophobic surfaces, and upon the formation of polydopamine via the *in-situ* polymerization, superhydrophilic micropatterns with well-controlled pattern dimension can be readily achieved on the superhydrophobic surfaces. The fog harvesting capability of these micropatterned superhydrophobic surfaces was then investigated. Compared with the uniformly superhydrophilic and superhydrophobic surfaces, the micropatterned superhydrophobic surfaces prepared by the current inkjet printing methods exhibited enhanced water collection efficiency. The method reported here is capable of facile large-scale patterning of superhydrophobic surface with high precision and superior pattern stability, thus represents a key step towards patterning superhydrophobic surfaces for practical applications.

Introduction

Water scarcity is the most severe problem in the semi-arid, desert regions, land scarce countries as well as countries of high economic activities,[1,2] where collecting atmospheric water, for example fog, has been well recognized recently as one of the important alternative methods for providing water source.[3-10] In this regard, one inspiration from nature is the unique fog basking capability of the *Stenocara* beetles, which helps the beetles to survive in the Namib Desert, one of the most arid area in the world.[3-5] Closer observation of the beetle's back reveals that it has a unique array of hydrophilic bumps, distributed on a superhydrophobic, wax-coated background, which allows for efficient condensation of water from fog-laden wind.[4] Motivated by this fog harvesting capability of the beetle, great efforts have been devoted to biomimetic preparation of the superhydrophobic surface patterned with the hydrophilic patches for the purpose of fog harvesting.[11-16] However, the current methods for creating such patterned surfaces mainly rely on mask-based strategy, where a pre-designed mask preparation is involved followed by a subsequent pattern transfer, which is multistep, indirect and expensive.[13-22] To produce stable hydrophilic micro-sized patterns on superhydrophobic substrates for practical applications, a direct method (i.e., one-step and thus mask-free) of depositing hydrophilic species in well-defined micropatterns[23,24] is still highly desired, but is nonexistent up to this point. This is so because of the following two reasons: (1) the ultralow surface energy of the superhydrophobic substrate surface greatly decreases the adhesion between the hydrophilic species and the surface, resulting in unstable deposition of the hydrophilic species.[23-28] (2) In addition, superhydrophobic surface entails rough surface structure and trapped in the interstices of the rough surface is air. Due to the presence of those discrete air pockets, water droplet sitting on such a solid-air composite surface interacts only with the small fraction of solid surface, which is widely known as Cassie's wetting state.[29,30] Therefore, in this case, both limited interaction area and adhesion between the hydrophilic species in the aqueous droplets and the superhydrophobic substrate make impossible of directly patterning superhydrophobic surfaces. Thus, a direct and general method to this end has to enhance the interaction strength (i.e., adhesion) between the hydrophilic species in the aqueous droplets and the superhydrophobic surface and to increase the contacting area of solid surface and liquid droplets.

In this regard, nature once more provides an insightful hint to aid us: marine mussels are promiscuous fouling organisms and have been shown to attach to virtually all types of inorganic and organic surfaces, including classically adhesion-resistant (low-surface-energy) materials such as Teflon.[31-33] Studies on bio-adhesive protein of many marine mussels discovered that it is the repeated dihydroxyphenylalanine (DOPA)-lysine motif that is responsible for mussel's high adhesion (i.e., high interaction strength) to low-surface-energy materials.[34-36] Recently, Lee and co-workers have identified that polydopamine has the similar chemical structure and thus functions to the bio-adhesive protein,[33] and further successfully demonstrated polydopamine formed via *in-situ* oxidative self-polymerization of dopamine could modify superhydrophobic surfaces and even obtained polydopamine patterned superhydrophobic surfaces based on mask-based soft-lithographic techniques.[17,18] These findings inspire us that depositing dopamine aqueous droplets followed by the *in-situ* formation of polydopamine would be a promising direct surface patterning method to produce stable hydrophilic micropatterns on superhydrophobic surfaces.

However, there stand other hurdles: (1) as discussed above, an aqueous dopamine droplet on a superhydrophobic surface conforms to Cassie's wetting behavior, under which limited interaction between the dopamine and contacting solid surface is resulted in, leading to inability to modify the solid surface in a controlled manner. Thus, to this end, instead of Cassie's wetting behavior, a Wenzel's wetting state[30,37] of the aqueous dopamine droplet with a high contact angle on the superhydrophobic surface is favorable and also beneficial for the controllable and precise deposition of dopamine solution droplets at pre-designated locations. Under Wenzel's wetting state, dopamine droplets penetrates into the rough structures of the superhydrophobic surface, displaces the air pockets, and thus maximize the interaction area of dopamine and the solid surface. (2) On the other hand, to obtain well-defined hydrophilic micropatterns on superhydrophobic surfaces in a direct method, small volume (nanoliter or even picoliter) droplet of hydrophilic species solution is deposited by means of point-by-point or line-by-line manner, which in turn leads to fast and uncontrolled evaporation of the solvent due to its high surface area exposed in air. This condition is unfavorable for stable and sufficient oxidative self-polymerization of dopamine as it requires a prolonged wet condition.[33] Therefore, inducing the transition from the Cassie's to Wenzel's wetting state of the dopamine droplets and slowing its fast evaporation on the superhydrophobic surface are two important concerns that need to be addressed for a successful direct micropatterning method.

Herein, we hypothesize that reducing surface tension of aqueous dopamine droplets would lead to a transition from Cassie's to Wenzel's wetting state and lowering its vapor pressure would prolong dopamine's self-polymerization on the superhydrophobic surface, which, once optimized, would result in a successful direct polydopamine micropatterning on superhydrophobic surfaces. Therefore, in this study, we optimized the droplet composition by delicately selecting water-miscible solvents with low surface tension and vapor pressure for the dopamine solution, and obtained a stable and prolonged Wenzel's microdroplets of the dopamine solution with a high contact angle on the superhydrophobic surface. As a proof of concept, inkjet printing is used here to directly print pre-designed micropatterns using dopamine solution with the optimized composition onto superhydrophobic surfaces. As a well-established and general patterning technology, inkjet printing has been widely accepted for a variety of industrial and scientific applications, on account of its ability to precisely deposit picoliter volumes of solution droplets in well-defined patterns.[38-41] The subsequent *in-situ* self-polymerization of dopamine in the microdroplets leads to stable superhydrophilic micropatterns of polydopamine on the superhydrophobic substrate. The micropatterned superhydrophbic surfaces prepared by the current inkjet printing method exhibit enhanced fog harvesting capability compared with the uniformly superhydrophilic and superhydrophobic surfaces. The method reported here is capable of facile large-scale patterning of superhydrophobic surface with high precision and superior pattern stability, and is suited for complicated pattern and thus it represents a key step towards patterning superhydrophobic surfaces for practical applications.

Experimental section

Materials

Dopamine hydrochloride, polystyrene granules (PS, 1~2 mm, Mw 350 000), 1H,1H,2H,2H-perfluorooctyltriethoxysilane (POTS), poly(ethyleneimine) (PEI, Mw. ~750 000), fluorescein sodium, rhodamine B, rhodamine B isothiocyanate, Trizma® base, ethanol, ethylene glycol, chloroform, $(NH_4)_2S_2O_8$, HCl, and NaOH were purchased from Sigma-Aldrich (St Louis, MO, USA). Hydrophobic PDMS-modified silica nanoparticles (diameter ca. 14 nm), Copper foil (thickness 1 mm, purity 99.99%), and polystyrene (PS) microsphere suspension (diameter ~10 µm, 2.5 wt%) were purchased from Alfa Aesar (Karlsruhe German). All these chemicals were used as received. Deioned (DI) water purified in a Milli-Q (Millipore, Billerica, MA, USA) system was used in all experiments.

Superhydrophobic surface preparation on glass slide substrate

1.0 g of the silica nanoparticles was dispersed in 30 mL of chloroform, and then 1.0 g of PS granules was dissolved in this dispersion by continuous stirring for 1 hour. The mixture was then spin-coated on the pre-cleaned glass slides at ca. 1500 rpm for 60 seconds. The coated glass slides were then transferred into an oven and calcinated for 2 hours at 600˚C to remove the organic component and fuse the silica nanoparticles together. To reduce the surface energy, the calcinated glass slides were coated with a semifluorinated silane of POTS by chemical vapor deposition to obtain superhydrophobic surfaces.[42]

Patterning superhydrophobic surface by the inkjet printing of the dopamine solution

A piezoelectric-based inkjet printer of Dimatix Materials Printer DMP-2800 (Fujifilm, Valhalla, NY, USA) was employed to print the dopamine solution onto the superhydrophobic glass slide surface. The Dimatix Materials Printer cartridge used produces 10 picoliter droplets. Freshly prepared dopamine solution (5.0 mg mL^{-1}) in tris buffer solution (10 mM, pH 8.5), ethanol, and ethylene glycol (1:1:1, v:v:v) was filled in the cartridge, and then inkjet printed on the superhydrophobic substrate with the pre-designed patterns at room temperature. The cartridge was placed 300 µm above the substrate for the printing process. After printing, the substrate was transferred to a sealed chamber, and kept at 50 ˚C for 36 hours to allow dopamine polymerization. Finally, the substrate was washed with copious ethanol and dried with nitrogen flow.

Fog harvesting measurement

The prepared substrates (~4.0 mm^2) were placed on a thermoelectric cooling module, and a simulated fog flow (~10 cm s^{-1}) was generated by a commercial humidifier and captured by the vertically placed substrate surfaces. The temperature and the relative humidity around the substrates were ~22˚C and 90~95%, respectively. The temperature of the substrates was maintained at ~4˚C by the cooling module, which is lower than the dew point of ~20˚C. Water collected by the surfaces was drained by gravity into a container placed under the sample. A digital optical microscope (Dino-Lite) was used to record the water condensation and movement behaviors. The weight of collected water was measured after one hour.

Characterizations

Scanning electron microscopy images were obtained on an FEI Quanta 600 scanning electron microscope (FEI Company, Hillsboro, OR, USA). Contact angle and sliding angle measurements were performed with a commercial contact angle system of OCA 35 (DataPhysics, Filderstadt, Germany) at ambient temperature using a 4 μL droplet as the indicator. The optical and fluorescent microscopic measurements were performed by a multipurpose zoom AZ100-M system (Nikon, Japan). X-ray photoelectron spectroscopy (XPS) measurements were recorded on an AXIS-NOVA instrument (Kratos Analytical Ltd, Manchester, UK) using a monochromatic Al Ka x-ray source (1486.6 eV). Survey spectra were collected using a pass energy of 160 eV and a step size of 1 eV. Pass energy of 20 eV and a step size of 0.1 eV were used for the high resolution spectra. The XPS analysis was performed with small spot analysis size of 110 μm×110 μm at a base pressure of $<1\times10^{-9}$ Pa. The lateral distribution of the elements on the surface was mapped using imaging-XPS. Charge neutralization was required for all samples. Binding energies were referenced to the C 1s binding energy of adventitious carbon contamination which was taken to be 285.0 eV for superhydrophobic surface, while the binding energy scale was referenced to the sp2 carbon component from polydopamine at 284.4 eV in the C 1s spectrum. The data were analyzed with commercially available software, CASAXPS. The individual peaks were fitted by a Gaussian (70%)–Lorentzian (30%) (GL30) function after Shirley type background subtraction. Digital images and videos were captured by using a Nikon COOLPIX P100 camera (Nikon, Japan).

Results and discussion

Our strategy of inkjet printing for the micropatterning of superhydrophobic surface is shown in Fig. 1a. The key step is to realize stable Wenzel's wetting behavior of deposited microdroplets of dopamine solution onto the superhydrophobic surfaces, while keeping their contacts effective and sufficient both in term of their contact area and time to ensure the sufficient oxidative self-polymerization and ultimately the stable hydrophilic patterning (Fig. 1b and 1c).

To test our hypothesis and obtain an optimized solution composition, a superhydrophobic surface was first prepared on glass slide substrate by depositing silica nanoparticles to obtain a rough surface followed by a fluorination process to decrease the surface energy (Electronic Supplementary Information, Fig. S1). The as-prepared superhydrophobic surface exhibited water contact angle of ca. 157˚ and sliding angle less than 1˚ (Table 1 and Fig. 2a and 2b), indicating a typical Cassie's wetting behavior.[29,30] Then, ethanol, a water-miscible and low-surface-tension solvent (surface tension, 22 mN m^{-1}) was first added into water, and the wetting behaviors of the liquid mixture with different fraction of ethanol on the superhydrophobic substrate were investigated, and the results are shown in Table 1. As the fraction of ethanol in the mixture increased, the contact angle decreased on the surface. Especially, for a mixture droplet of water and ethanol with a ratio of 1:1 (v:v), a contact angle of ca. 134˚ was measured, and most importantly the droplet firmly pinned on the surface, without detachment even when the substrate was reversed to a upside down position, indicating a Wenzel's wetting behavior of such a mixture liquid droplet on the surface.[30,37] These results have clearly demonstrated that by varying the fraction of low-surface-tension solvent (i.e., ethanol) in water, a transition of the wetting behavior from Cassie's to Wenzel's state is achieved for mixture droplet on the superhydrophobic surface.

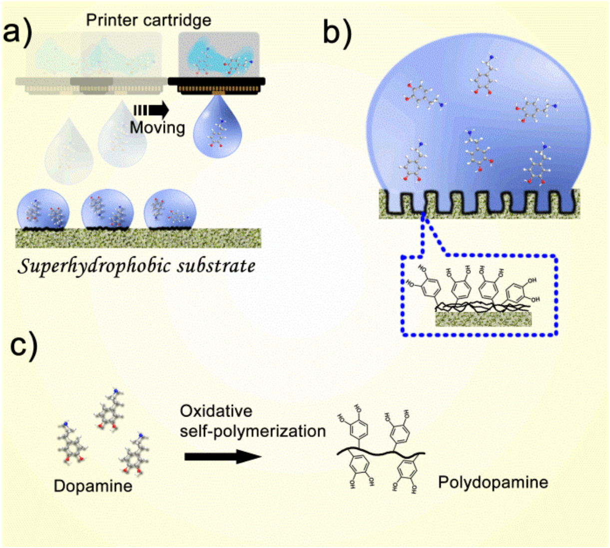

Fig.1 (a) Scheme of the inkjet printing method for the micropatterning of superhydrophilicity on superhydrophobic surfaces. **(b)** The Wenzel's wetting behavior of the deposited microdroplet of dopamine solution on the superhydrophobic surface. **(c)** Schematic illustration for formation of polydopamine by the oxidative self-polymerization of dopamine.

Table 1 Wetting behaviors of the liquid droplets on the superhydrophobic substrate. By increasing the low-surface-tension liquid of ethanol in water, the contact angle of the droplet decreased, and the adhesion of the droplet to the superhydrophobic surface increased.

	Water	Water: Ethanol (3:1)	Water: Ethanol (2:1)	Water: Ethanol (1:1)	Water: Ethanol (1:2)	Ethanol
Contact angle (˚)	157	155	146	134	15	0
Sliding Angle (˚)	<1	3	7	NA[a)]	NA[a)]	NA[a)]

[a] Liquid droplets were pinned on the surfaces with high adhesion, and no sliding behaviors were observed during the tilting of the substrates.

On the other hand, for the purpose of lowering the vapor pressure and thus slowing down the evaporation of dopamine solution microdroplets on the superhydrophobic surface, another solvent of ethylene glycol with a high boiling point (197.3^{o}C), a low

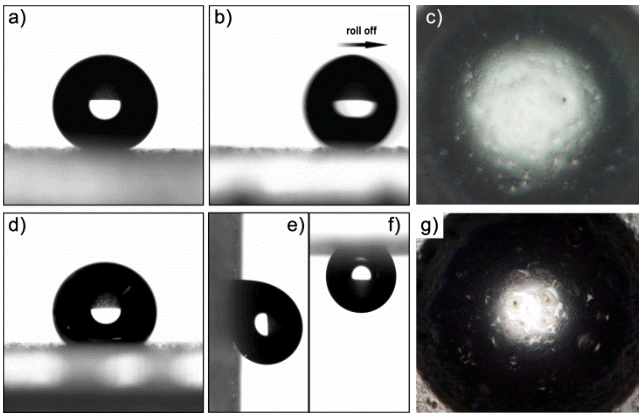

Fig.2 **(a)** Shape of a water droplet on the superhydrophobic surface (contact angle is ca. 157°). **(b)** Snapshot from the contact angle measurement video showing the rolling of the water droplet off the superhydrophobic substrate upon slight tilt of the substrate, with a sliding angle less than 1°. **(c)** Top-view optical image of the interface between the water droplet and the superhydrophobic surface. Shapes of tri-solvent droplet of water, ethanol, and ethylene glycol (1:1:1) (in the absence of dopamine) on the superhydrophobic surfaces with different tilt angle: **(d)** 0° (contact angle is ca. 130°), **(e)** 90°, and **(f)** 180°. **(g)** Top-view optical image of the interface between tri-solvent droplet and the superhydrophobic surface.

vapor pressure (0.06 mmHg at room temperature), and a low surface tension (47 mN m^{-1}) was selected to add in the solvent system. Ultimately, a water-ethanol-ethylene glycol tri-solvent system with the volume ratio of 1:1:1 was chosen as the solvent for the preparation of dopamine solution for directly micropatterning superhydrophobic surface. As can be seen in Fig. 2d, the tri-solvent droplet in the absence of dopamine exhibited a contact angle of ca. 130° and high adhesion to the superhydrophobic surface. Fig. 2e and 2f show that even when the substrate was perpendicularly and invertedly placed, the droplet still firmly adhered to the surface, indicating the Wenzel's wetting behavior.[30,37] To directly prove the Wenzel's wetting behavior of the tri-solvent droplet on the superhydrophobic surface, carried out was the top-view episcopic illumination microscopic observation of the interface between liquid droplet and the superhydrophobic surface. In this method, the air pockets in the nanostructures under a liquid droplet can be observed due to the light-reflection difference between the air-liquid interface and the liquid-solid interface. The high light reflection (bright region) observed under the droplets is from the interface between the liquid and the air, while the dark region is due to the low reflection at the liquid-solid interface.[43-45] For the pure water droplet on the superhydrophobic surface, as shown in Fig. 2c, bright region occupied the majority of the contacting area, demonstrating the continuous air plastron under the water droplet and confirming its Cassie's wetting state. While for the tri-solvent droplet of water, ethanol, and ethylene glycol, only sparse bright regions could be observed at the interface between the liquid droplet and the same superhydrophobic surface (Fig. 2g), suggesting that most of the air pockets were displaced from the interface, and sufficient and effective contact between the liquid droplet and the solid surface was achieved. This result together with the high adhesion of the tri-solvent droplet to the superhydrophobic surface confirms the Wenzel's wetting state. It should be noted that the dopamine solution prepared by the tri-solvent system exhibited very similar wetting behavior to that of the tri-solvent droplet (Electronic Supplementary Information, Fig. S2), indicating the negligible influence of dopamine on surface tension of the tri-solvent system.

Having confirmed the Wenzel's wetting of the tri-solvent droplet on the superhydrophobic surface, the surface modification by polydopamine in such tri-solvent system was then tested. The superhydrophobic substrate was immersed into the bulk dopamine solution prepared by the tri-solvent system and allowed for enough time (i.e., 36 hours) for dopamine to polymerize. After the polydopamine coating formation via the oxidative polymerization of dopamine, the treated surface turned superhydrophilic, with water contact angle being 0° (i.e., water droplet completely spreading over the surface within 0.2 s, Fig. 3a-3c). The formation of the polydopamine coating was also confirmed by X-ray photoelectron spectroscopy (XPS) measurement (Fig. 3d and Electronic Supplementary Information Fig. S3), which provides a direct evidence for the surface elemental composition and distribution and is commonly used to demonstrate the formation of polydopamine.[17,33,46] As shown in Fig. 3d1, the N 1s signal was almost absent for the unmodified superhydrophobic glass substrate. While for polydopamine modified area, the nitrogen peak appeared (Fig. 3d2). The N 1s peak was fitted with three components located at 401.5, 399.9, and 398. 4 eV, which can be assigned to primary (R-NH_2), secondary (R-NH-R), and tertiary (=N-R) amine functionalities, respectively. The dominant secondary amine component (R-NH-R) situated at 399.9 eV is a signature of formation of polydopamine.[46] These results confirmed that in the tri-solvent system, dopamine undergoes oxidative self-polymerization, forms polydopamine, which modifies the superhydrophobic surface.

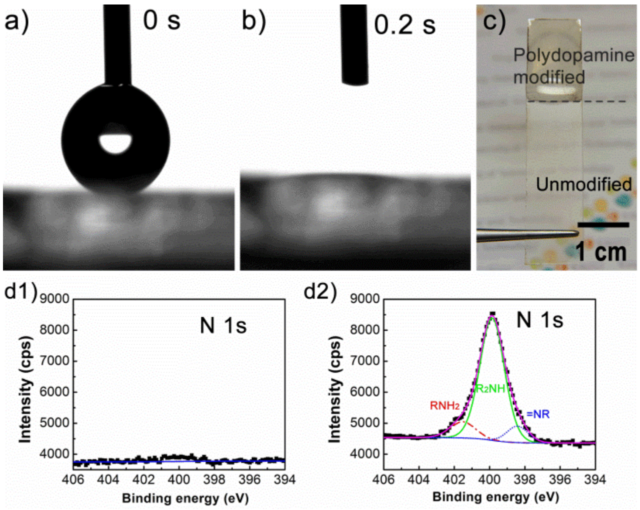

Fig.3 **(a)** and **(b)** Snapshots from the contact angle measurement video showing the wetting behavior of a water droplet on the polydopamine modified superhydrophobic glass slide. After the modification of polydopamine, a superhydrophilic surface was achieved with a complete spreading (within less than 0.2 s) of the water droplet, which was the result of the combination of the hydrophilic property of the deposited polydopamine and the rough surface structure. **(c)** Photo of polydopamine partially modified superhydrophobic glass slide. Water wetted the polydopamine modified region (upper part of the substrate), but couldn't spread to the lower region due to its extremely water-repellent property.

High-resolution XPS spectra of N 1s recorded from the unmodified area **(d1)** and polydopamine modified area **(d2)** of the substrate.

Based on the successful confirmation of both the Wenzel's wetting state and formation of polydopamine on the superhydrophobic surface, the inkjet printing of the tri-solvent dopamine solution was then conducted. More specifically, the freshly prepared dopamine solution was filled in a printer cartridge and then printed on the superhydrophobic surface in picoliter-volume droplets. Fig. 4a shows the optical microscopic image of the as-printed square array of the dopamine solution with the feature size of ca. 200 µm. Upon printing, the dopamine droplets firmly adhered to the pre-designated locations on the superhydrophobic substrate without any detachment, even when the substrate was perpendicularly and invertedly placed. The superhydrophobic substrate with the printed dopamine solution droplets was then stored in a sealed chamber for 36 hours, allowing the oxidative self-polymerization of dopamine to take place. The modified surface was then rinsed with copious ethanol to remove the residue solvents and unattached polydopamine before drying with nitrogen flow. As revealed in the optical microscopic photograph in Fig. 4b, after the above treatments, the polydopamine pattern of square array on the surface was clearly observed and the size of polydopamine pattern (ca. 200 µm) was the same as that of the printed precursor dopamine droplet in Fig. 4a. The as-prepared polydopamine pattern on the superhydrophobic surface is quite stable, and can withstand intensively organic solvents (specifically, acetone and ethanol) and water flushing. Furthermore, to evaluate the stability of the polydopamine micropatterns, a simulated high speed wind (40~50 m s^{-1}) generated by compressed air was blown onto the surfaces, and after treatment, the superhydrophilicity of the polydopamine coating (patterns) remained unchanged, indicating the high adhesion to the underneath superhydrophobic substrates. Besides, we also found that the polydopamine micropatterns are stable after storage in ambient condition for one year. These results indicate that the polydopamine micropatterns on the superhydrophobic surface prepared by the current inkjet printing method are stable and promising for practical application. Fig. 4c and 4d show the scanning electronic microscopic (SEM) images of the central and edge parts of the polydopamine pattern, respectively. It can be observed that the formed polydopamine coating uniformly covered the superhydrophobic surface, with nanoparticle with sizes from 50 nm to 100 nm clearly observable. These nanoparticles were the silica nanoparticles coated with polydopamine and the polydopamine nanoparticles formed during the oxidative polymerization process. These hydrophilic polydopamine nanoparticles due to the presence of the polar functional groups (i.e. hydroxyl and amine groups) on the patterned area increased the surface roughness, and thus enhanced the hydrophilicity of the polydopamine patterns, leading to superhydrophilicity (Fig. 3a-c). The thickness of the polydopamine coating is around 45 nm, as revealed by the edge of the pattern in Fig. 4d. By using the current inkjet printing method, micropatterns of polydopamine with various feature sizes can be readily prepared (Electronic Supplementary Information, Fig. S3). We also found that the smallest pattern and separation distance created by this inkjet printing method based on the current printer was around 50 µm and 50~100 µm, respectively, which is comparative to what the existing mask-based method can produce in terms of preparation of patterned wettability.[13-21] We believe that by employing other direct patterning techniques such as dip-pen nanolithography[47] or high resolution inkjet printer, micropatterns with micro or even nanoscale feature sizes could be readily obtained.

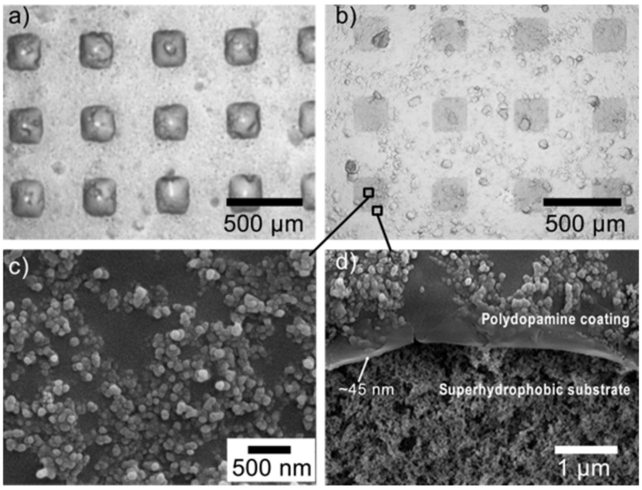

Fig.4 (a) Optical microscopic photograph of the as-printed dopamine droplet on the superhydrophobic surface. **(b)** Optical microscopic photograph of the polydopamine patterns on the surface. The particulates observed in the optical microscopic images are the micro-sized aggregates of the deposited silica nanoparticles, which contributed to the rough surface and were indispensable for the superhydrophobicity of the substrate. **(c)** and **(d)** SEM images of the formed polydopamine patterns.

It is worth mentioning that the high boiling point (low vapor pressure) of ethylene glycol is critically important for the direct micropatterning (inkjet printing) strategy to work. It was found that when the inkjet printing of dopamine solution was conducted without ethylene glycol (i.e., only di-solvent of water and ethanol at ratio of 1:1), no liquid droplets could be observed on the printed area of the superhydrophobic substrate, and only some discretely distributed dry powders (Electronic Supplementary Information, Fig. S4) were seen. Presumably, this is because of the high vapor pressure of water and ethanol, which evaporated quickly during and after printing, leaving behind only the solutes on the substrates. The fast evaporation of the solvents leads to inability of forming uniform polydopamine coating on the superhydrophobic surface. This result confirms the critical role of ethylene glycol in the dopamine solution.

To verify the successful patterning of the superhydrophobic surface, the substrate with the polydopamine micropatterns was immersed in water and then withdrawn, and it could be clearly observed that there were tiny discrete water droplets exclusively adhering to the polydopamine modified patches, isolated by the non-modified regions (Fig. 5a). Furthermore, for the purpose of facilitated observation, fluorescein sodium was added to water, and a fluorescent microscopic imaging was taken to characterize the water droplets immediately after withdrawing the substrate from the water. As can be seen from Fig. 5b, significant green fluorescence was clearly visible only in the polydopamine patterned area, which confirms that the water droplets, labeled with fluorescein sodium, attached only on the hydrophilic areas, confirming the successful patterning of the superhydrophobic surface. Using the patterned surfaces, hydrophilic molecules and microspheres can be selectively immobilized on the pre-designated area of the polydopamine patterns. Fig. 5c and 5d show the fluorescent microscopic photographs of the rhodamine B molecule and rhodamine B-labeled polystyrene (PS) microspheres (diameter ~10 μm) that were selectively immobilized on the patterned superhydrophobic surface (Electronic Supplementary Information, experimental details). It should be noted that the current inkjet printing method is versatile method and is able to directly pattern a variety of superhydrophobic surfaces. One example is the micropatterning of superhydrophobic copper foil substrate (Electronic Supplementary Information, experimental details and Fig. S5).

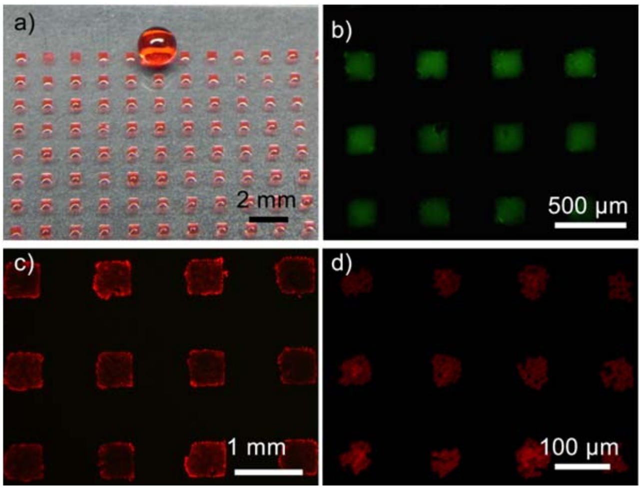

Fig.5 **(a)** Photograph showing water droplets on the polydopamine patterns (500-μm square) of the superhydrophobic substrate, after the substrate was taken out from water. The water was stained with aqueous red ink for a facilitated observation. A large water droplet (6 μL) was also placed on the surface for comparison, and it could not wet the surface. **(b)** Fluorescent microscopic image of the patterned superhydrophobic surface with a square array of polydopamine after dipping in water with fluorescein sodium. The size of the inkjet-printed polydopamine patterns was ca. 200 μm. **(c)** and **(d)** Fluorescent microscopic images of rhodamine B and PS microspheres (labeled with rhodamine B) immobilized on the patterned superhydrophobic surfaces. **(c)** Square array with the size of ca. 500 μm. **(d)** Square array with the size of ca. 50 μm.

Having confirmed the successful micropatterning of the superhydrophobic surfaces, we then investigated the fog harvesting performance by the polydopamine micropatterned superhydrophobic surfaces prepared by the current inkjet printing method. Fig. 6a shows the schematic setup for the fog harvesting system. In more details, a simulated fog flow was generated by a commercial humidifier and captured by the condensing substrate. The substrate was mounted on a cooling module, which maintained the substrate temperature at 4 °C constantly, sufficiently lower than the dew point. Water condensed on the substrates was drained, by gravity, into a collection container below. Fig. 6b shows the comparison of the water collection efficiency of five different substrates: superhydrophilic glass substrate (with a water contact angle less than 5°), superhydrophobic glass substrate, polydopamine patterned superhydrophobic substrate with pattern size being ~500 μm and pattern separation ~1000 μm, polydopamine patterned superhydrophobic substrate with pattern size being ~200 μm and pattern separation ~400 μm, polydopamine patterned superhydrophobic substrate with pattern size being ~200 μm and pattern separation ~1000 μm. Clearly, the superhydrophilic surface showed a water collection efficiency of ~14.9 mg cm^{2} h^{-1}, which was the lowest among the five tested substrates, while the uniformly superhydrophobic surface achieved a water collection efficiency of ~30.0 mg cm^{2}h^{-1}. In comparison, enhanced water collection efficiency was observed on all three polydopamine micropatterned superhydrophobic surfaces, ranging from ~33.2 to 61.8 mg cm^{2}h^{-1}. Especially, for the micropatterned substrate with a pattern size at ~500 μm and separation distance ~1000 μm, it exhibited the highest efficiency of ~61.8 mg cm^{2}h^{-1}, which was about 4 times that of the superhydrophilic surface.

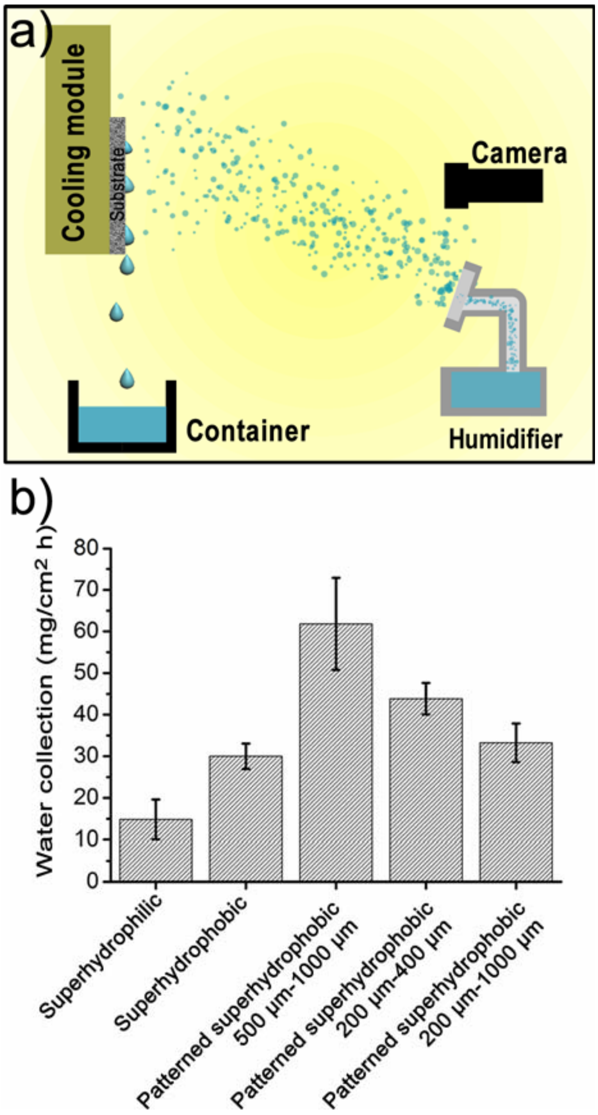

Fig.6 **(a)** Experimental setup of water collection system from fog. **(b)** Water collection efficiency by five different surfaces.

To better understand the fog harvesting behaviours of these substrates, an optical microscopic imaging was conducted to record the water collection processes on these surfaces. As shown in Fig. 7a, for the uniformly superhydrophilic surface, water droplets, once condensed, immediately spread out over the surface, and a thin water film was formed within a short period of time, which is known as film-wise condensation.[48] In contrast, as shown in Fig. 7b, tiny spherical water droplets were formed and captured on the uniformly superhydrophobic surface and the droplets gradually merged into big ones. As the sizes of these droplets grew beyond certain threshold, the droplets became unstable, and rolled off the superhydrophobic surface due to the gravity force. Compared with the film-wise condensation on the superhydrophilic surface, (1) the drop-wise condensation of superhydrophobic surface allows for a more efficient heat transfer, as the water film has a higher interfacial thermal resistance; (2) the self-clearing of the droplets from the superhydrophobic surfaces enables continuous nucleation and growth of new droplets, leading to enhanced the water collection.[48-52]

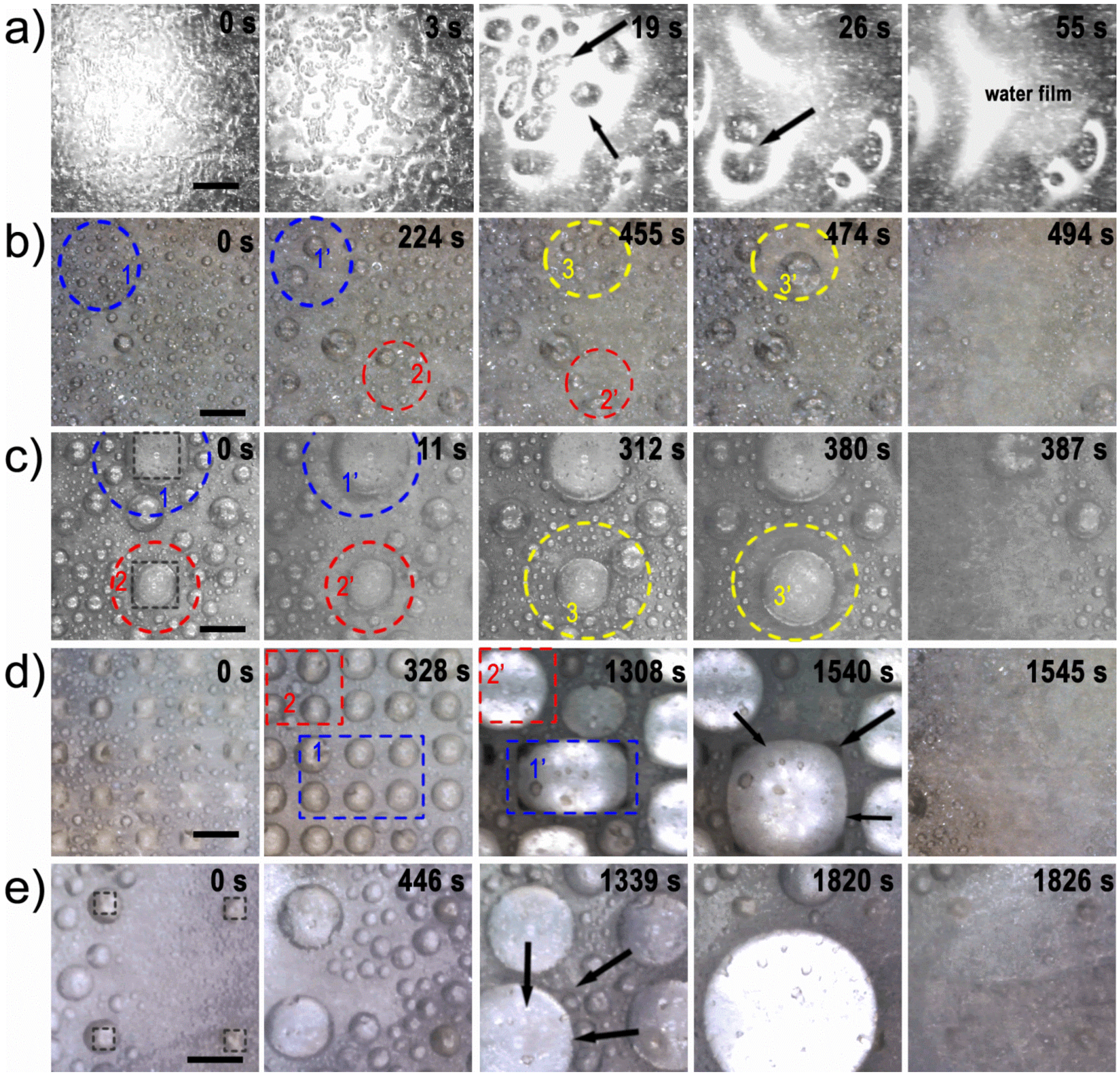

Fig.7 Water collection processes on various kinds of surfaces. **(a)** On superhydrophilic surface, water droplets spread over the surface, and form thin water film quickly, as the arrow indicated. **(b)** On superhydrophobic surface, the captured tiny droplets coalesce randomly, as indicated by the dash circles. As the sizes of these droplets grow beyond certain threshold, the droplets roll off the superhydrophobic surface. **(c)** On superhydrophobic surface with ~500 µm polydopamine patterns and ~1000 µm separation, **(d)** on superhydrophobic surface with ~200 µm polydopamine patterns and ~400 µm separation, and **(e)** superhydrophobic surface with ~200 µm polydopamine patterns and ~1000 µm separation, tiny droplets spontaneously move and coalesce into the superhydrophilic polydopamine micropatterns, as indicated by the dashed circles and arrows. Some of the polydopamine micropatterns are outlined with black dashed dots. All scale bars are 500 µm.

On the other hand, as shown in Fig. 7c-e, the condensation and capture of tiny water droplets captured on the superhydrophobic regions on the micropatterned surfaces were also observed, but once formed, these droplets preferentially moved toward the polydopamine modified superhydrophilic regions, driven by the wettability differences, and subsequently coalesced into bigger droplets there. As the droplets in the superhydrophilic regions grew beyond certain threshold, they were cleared off the surface by gravity. From a water collection point of view, a desirable surface promotes (1) droplet nucleation and (2) droplet removal simultaneously, a seemingly fighting pair. Thus, there have to be well-selected tipping point when these two properties are integrated in one surface, as the droplet nucleation requires hydrophilicity, while droplet removal is benefited from superhydrophobicity.[48-52] The micropatterned superhydrophobic surfaces in this study integrated these two properties into one surface, thus leading to their better water collection performance than their uniformly superhydrophilic and superhydrophobic counterparts. Moreover, our results expectedly revealed that the micropatterned superhydrophobic surface with a similar pattern dimension of that of the desert beetle's back (i.e., ~500 µm pattern size and ~1000 µm separation distance), exhibited the highest water collection efficiency among all. We also found that the polydopamine patterned superhydrophobic substrate with pattern size being ~200 µm and pattern separation ~1000 µm showed water collection efficiency only slighly higher than that of the uniformly superhydrophobic surface. This is probably because of the relatively small superhydrophilic area fraction (~5%), compared with those of the polydopamine patterned superhydrophobic substrates with pattern size being ~200 µm, pattern separation ~400 µm (16%), and pattern size being ~500 µm, pattern separation ~1000 µm (~25%). The attempt to further enhance the water collection efficiency on these patterned surfaces is currently underway in our group.

Conclusion

In conclusion, we have reported a bio-inspired method for the direct preparation of superhydrophilic micropatterns on superhydrophobic surface based on a facile inkjet printing strategy. By directly depositing microdroplets of dopamine solution with an optimized solvent system, followed by *in-situ* formation of polydopamine, superhydrophilic micropatterns could be readily obtained on the superhydrophobic surface. The micropatterned superhydrophbic surfaces prepared by the current inkjet printing method exhibit enhanced water collection capability compared with the uniformly superhydrophilic and superhydrophobic surfaces. We envision that with this convenient strategy, the design and large-scale fabrication of patterned superhydrophobic surface would be greatly facilitated, which opens up a new avenue for the patterned superhydrophobic surface in practical applications, such as fog harvesting and water condensenation/collection in thermal desalination processes.

Acknowledgements

The authors thank KAUST CRG2 for funding. The authors also thank Prof. Karl Leo and Dr. Silvano Del Gobbo for providing access to the Dimatix Materials Printers in the KAUST Solar & Photovoltaics Engineering Research Center, and Dr. Adam Roberts from Kratos Analytical Ltd. for the help with the XPS measurements.

Notes and references

[a] *Biological and Environmental Sciences and Engineering Division, Water Desalination and Reuse Center, King Abdullah University of Science and Technology, Thuwal 23955-6900, Saudi Arabia.*
E-mail: peng.wang@kaust.edu.sa
[b] *Imaging and Characterization Laboratory, King Abdullah University of Science and Technology, Thuwal 23955-6900, Saudi Arabia.*

1 Q. Schiermeier, *Nature*, 2014, **505**, 10–11.
2 M. M. Pendergast and E. M.V. Hoek, *Energy Environ. Sci.*, 2011, **4**, 1946-1971.
3 W. J.Hamilton and M. K. Seely, *Nature*, 1976, **262**, 284−285.
4 A. R. Parker and C. R. Lawrence, *Nature*, 2001, **414**, 33-34.
5 T. Nørgaard and M. Dacke, *Front. Zool*., 2010, **7**, 23−30.
6 J. D. D. Rivera, *Atmos. Res.*, 2011, **102**, 335−342.
7 J. Ju, H. Bai, Y. Zheng, T. Zhao, R. Fang and L. Jiang, *Nat. Commun*., 2012, **3**, doi: 10.1038/ncomms2253.
8 Y. Zheng, H. Bai, Z. Huang, X. Tian, F.-Q. Nie, Y. Zhao, J. Zhai and L. Jiang, *Nature*, 2010, **463**, 640-643.
9 C. R. Tracy, N. Laurence and K. A. Christian, *Am. Nat.*, 2011, **178**, 553−558.
10 I. Lekouch, M. Muselli, B. Kabbachi, J. Ouazzani, I. Melnytchouk-Milimouk and D. Beysens, *Energy*, 2011, **36**, 2257−2265.
11 L. Zhai, M. C. Berg, F. C. Cebeci, Y. Kim, J. M. Milwid, M. F. Rubner and R. E. Cohen, *Nano Lett.*, 2006, **6**, 1213–1217.
12 S.C. Thickett, C. Neto and A. T. Harris, *Adv. Mater.*, 2011, **23**, 3718–3722.
13 H. Bai, L. Wang, J. Ju, R. Z. Sun, Y. M. Zheng and L. Jiang, *Adv. Mater.*, 2014, **26**, 5025–5030.
14 A. Lee, M.-W. Moon, H. Lim, W.-D. Kim and H.-Y. Kim, *Langmuir*, 2012, **28**, 10183–10191.
15 R. P. Garrod, L. G. Harris, W. C. E. Schofield, J. McGettrick, L. J. Ward, D. O. H. Teare and J. P. S. Badyal, *Langmuir*, 2007, **23**, 689–693.
16 C. Dorrer and J. Rühe, *Langmuir*, 2008, **24**, 6154–6158.
17 S. M. Kang, I. You, W. K. Cho, H. K. Shon, T. G. Lee, I. S. Choi, J. M. Karp and H. Lee, *Angew. Chem., Int. Ed.*, 2010, **49**, 9401–9404.
18 I. You, S. M. Kang, S. Lee, Y. O. Cho, J. B. Kim, S. B. Lee, Y. S. Nam and H. Lee, *Angew. Chem., Int. Ed.*, 2012, **51**, 6126–6130.
19 T. Ishizaki, N. Saito and O. Takai, *Langmuir*, 2010, **26**, 8147–8154.
20 D. Zahner, J. Abagat, F. Svec, J. M. J. Fréchet and P. A. Levkin, *Adv. Mater.*, 2011, **23**, 3030–3034.
21 U. Manna, A. H. Broderick and D. M. Lynn, *Adv. Mater.*, 2012, **24**, 4291–4295.
22 O. S. Kwon, S. H. Lee, S. J. Park, J. H. An, H. S. Song, T. Kim, J. H. Oh, J. Bae, H. Yoon, T. H. Park and J. Jang, *Adv. Mater.*, 2013, **25**, 4177–4185.
23 J. S. Li, E. Ueda, A. Nallapaneni, L. X. Li and P. A. Levkin, *Langmuir*, 2012, **28**, 8286–8291.
24 Y. k. Lai, F. Pan, C. Xu, H. Fuchs and L. F. Chi, *Adv. Mater.*, 2013, **25**, 1682–1686.
25 A. Lafuma and D. Quéré, *Nat. Mater.*, 2003, **2**, 457-460.
26 T. L. Sun, L. Feng, X. F. Gao and L. Jiang, *Acc. Chem. Res.*, 2005, **38**, 644–652.
27 X. Zhang, F. Shi, J. Niu, Y. G. Jiang and Z. Q. Wang, *J. Mater. Chem.*, 2008, **18**, 621-633.
28 X. M. Li, D. Reinhoudt and M. Crego-Calama, *Chem. Soc. Rev.*, 2007, **36**, 1350-1368.
29 A. B. D. Cassie and S. Baxter, *Trans. Faraday Soc.*, 1944, **40**, 546-551.
30 S. Wang and L. Jiang, *Adv. Mater.*, 2007, **19**, 3423–3424.
31 J. H. Waite and M. L. Tanzer, *Science*, 1981, **212**, 1038–1040.
32 G. A. Young and D. J. Crisp, in *Adhesion*, ed. K. W. Allen, Applied Science, London, 1982, Vol. 6.
33 H. Lee, S. M. Dellatore, W. M. Miller and P. B. Messersmith, *Science*, 2007, **318**, 426-430.
34 J. H. Waite and X. X. Qin, *Biochemistry*, 2001, **40**, 2887–2893.

35 M. Yu, J. Hwang and T. J. Deming, *J. Am. Chem. Soc.*, 1999, **121**, 5825-5826.

36 H. Lee, N. F. Scherer and P. B. Messersmith, *Proc. Natl. Acad. Sci. U.S.A.*, 2006, **103**, 12999-13003.

37 R. N. Wenzel, *Ind. Eng. Chem.*, 1936, **28**, 988-994.

38 E. Tekin, P. J. Smith and U. S. Schubert, *Soft Matter*, 2008, **4**, 703-713.

39 M. Singh, H. M. Haverinen, P. Dhagat and G. E. Jabbour, *Adv. Mater.*, 2010, **22**, 673–685.

40 Y. Diao, L. Shaw, Z. Bao and S. C. B. Mannsfeld, *Energy Environ. Sci.*, 2014, **7**, 2145-2159.

41 W.-K. Oh, S. Kim, K.-H. Shin, Y. Jang, M. Choi and J. Jang, *Talanta*, 2013, **105**, 333-339.

42 Y. Li, L. Li and J. Q. Sun, *Angew. Chem., Int. Ed.*, 2010, **49**, 6129-6133.

43 C. Luo, X. L. Zuo, L. Wang, E. G. Wang, S. P. Song, J. Wang, J. Wang, C. H. Fan and Y. Cao, *Nano Lett.*, 2008, **8**, 4454-4458.

44 C. Luo, H. Zheng, L. Wang, H. Fang, J. Hu, C. Fan, Y. Cao and J. Wang, *Angew. Chem., Int. Ed.*, 2010, **49**, 9145-9148.

45 J. Gao, X. Yao, Y. Zhao and L. Jiang, *Small*, 2013, **9**, 2515–2519.

46 R. A. Zangmeister, T. A. Morris and M. J. Tarlov, *Langmuir*, 2013, **29**, 8619-8628.

47 R. D. Piner, J. Zhu, F. Xu, S. Hong and C. A. Mirkin, *Science*, 1999, **283**, 661-663.

48 V. P. Carey, *Liquid-Vapor Phase-Change Phenomena: An Introduction to the Thermophysics of Vaporization and Condensation Processes in Heat Transfer Equipment*, Hemisphere, Washington, D. C, USA, 1992.

49 C. Graham and P. Griffith, *Int. J. Heat Mass Transfer*, 1973, **16**, 337-346.

50 J. Feng, Z. Q. Qin and S. H.Yao, *Langmuir*, 2012, **28**, 6067−6075.

51 X. M. Chen, J. Wu, R. Y. Ma, M. Hua, N. Koratkar, S. H. Yao and Z. K. Wang, *Adv. Funct. Mater.*, 2011, **21**, 4617–4623.

52 N. Miljkovic, R. Enright, Y. K Nam, K. Lopez, N. Dou, J. Sack and E. N. Wang, *Nano Lett.*, 2013, **13**, 179–187.

Table of Contents Entry:

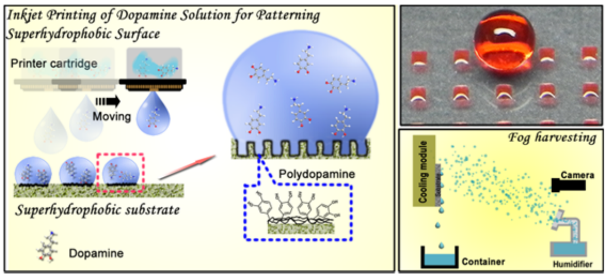

Direct micropatterning of superhydrophilicity on superhydrophobic surfaces is achieved by inkjet printing a mussel-inspired ink of dopamine solution on the superhydrophobic surface, followed by the formation of polydopamine via the *in-situ* polymerization. The micropatterned superhydrophobic surfaces exhibit enhanced fog harvesting efficiency.